

LASER PROCESSING OF POLYCRYSTALLINE DIAMOND, TUNGSTEN CARBIDE AND A RELATED COMPOSITE MATERIAL

Paul M Harrison, Matthew Henry, Michael Brownell

Powerlase Ltd, Imperial House, Link 10, Napier Way,
Crawley, West Sussex, RH10 9RA, UK

Abstract

There are numerous industrial uses of super hard materials such as polycrystalline diamond, natural diamond and Tungsten Carbide. These include tooling for mechanical processing as well as robust substrates for microelectronics in extreme environment applications. Processing these materials has presented a perennial problem for engineers. In this paper cutting and milling of these materials is investigated using high average power nanosecond pulsed diode pumped solid-state lasers. The results are investigated with regard to developing models for nanosecond pulse laser milling. It is found that it is possible to process these materials at superior rates to conventional technologies, achieving comparable quality without the issues of tool wear and lubrication to contend with. It is also determined that this technology can both cut and mill these materials in concurrent processing – offering new flexibility for manufacturing design.

1. Introduction

Recent advances in industrial diode pumped solid state lasers (DPSSLs) have resulted in new possibilities for materials processing applications involving super hard materials such as polycrystalline diamond (PCD) and tungsten carbide (WC). This new class of DPSSL combines high average powers, nanosecond pulse widths and superior beam quality to achieve new operating conditions and processing results. DPSSLs also offer a combination of good beam quality, high efficiency, rugged construction and long diode lifetime. This makes them a very attractive option to industries seeking an advantage in cutting edge manufacturing on both the macro and micro scale¹.

PCD is a synthetic, extremely tough, intergrown mass of randomly orientated diamond particles in a metal matrix. It is produced by sintering together selected diamond particles at high pressure and temperature. The sintering process is rigidly controlled within the

diamond stable region and an extremely hard and abrasion resistant structure is produced.

Polycrystalline diamond cutting tool blanks can be regarded as a composite material that combines the hardness abrasion resistance and thermal conductivity of diamond with the toughness of WC². These properties are best utilised in cutting tools for machining a wide variety of materials as well as in wear part applications, where they contribute to improved tool lifetime and offer additional technological advantages such as process reliability and more accurate machining tolerances.

PCD cutting tools are typically used to process non-ferrous metals, wood³ and rubber. The PCD blanks are cut to shape and brazed into individual holders which are assembled into a cutting tool, often with multiple PCD cutting teeth per tool. During the life of the tool the cutting edges wear down (although at a slower rate than traditional cutting tools), which necessitates sharpening of the cutting edges of the PCD teeth. If this is not done then dimensional tolerances are increased and cutting quality is lowered. Therefore, laser processing of PCD cutting tool blanks has two applications: cutting the initial tool shape and maintaining the tool sharpness.

As shown in Table 1, PCD has good compressive strength and heat conductivity. The hardness of PCD is inferior only to that of single crystal diamond³. The wear resistance of PCD has been shown to be superior to both cemented carbide and high speed steel (HSS), making it an outstanding choice for cutting tools.

This paper examines the Nd:YAG DPSSL processing of polycrystalline diamond cutting tool blanks, which are a lamina composite of PCD and WC. Industrial sample discs with polycrystalline diamond on one side and tungsten carbide on the other are used for these trials. This allows the characterisation of each material through laser milling and afterwards the

piercing and cutting of the composite material. Laser milling of PCD and WC is investigated to determine the material ablation characteristics and removal rates. The results are compared to previously published process modelling and experimental work⁴. Laser cutting of PCD cutting tool blanks is then investigated to establish the cutting mechanism and to determine the parameters for high quality cutting. The experimental work of this paper was performed using the Starlase range of lasers which is manufactured exclusively by Powerlase Ltd, UK.

| | Polycrystalline Diamond | Tungsten Carbide | Stainless Steel Grade 316 |
|---|---------------------------|------------------|---------------------------|
| Density [g cm^{-3}] | 3 to 4 [†] | 16 | 8 |
| Thermal Conductivity [$\text{W m}^{-1} \text{K}^{-1}$] | 540 | 100 | 16 |
| Modulus of Elasticity [GPa] | 749 to 953 [†] | 680 | 193 |
| Compressive Yield Stress [MPa] | 1900 to 6900 [†] | 2683 | 205 |
| Vickers Hardness [kg mm^{-2}] | 5098 | 1730 | 228 |
| Melting Point [K] | 1530 ^{††} | 2850 | 1400 |
| [†] These values depend on the grade of PCD ^{††} This is complex since PCD is a composite material | | | |

Table 1: Comparison of material properties of polycrystalline diamond, tungsten carbide and stainless steel^{2,3,5}.

2. Milling Trials

Laser milling trials were performed on the constituent materials separately. The results of these trials are presented in the following sections.

The laser milling tests used a Starlase AO2 Nd:YAG Q-switched DPSSL at the fundamental wavelength of 1064 nm. This pulsed laser offers average powers up to 220 W at a range of repetition rates and pulse durations between 3 to 50 kHz and 20 to 200 ns respectively. The output beam power is varied using a proprietary attenuator unit and then collimated with a Galilean telescope and directed into a galvanometric scanner (ScanLab HurryScan25).

During the course of the tests the scanner was fitted with an 80 mm focal length f-theta telecentric objective lens with a working target area of 25x25 mm which produced at best focus a $\text{Ø}160\mu\text{m}$ focal spot. All of the processing work was performed in air at standard atmospheric conditions and no gas assist was used.

Samples were analysed using a Nikon LM1500 optical microscope with a PC interface via a 12 megapixel camera into Lucia G software. This software allowed microscopic measurements to be made against a Nikon standard. Depth measurements were made using a Mitutoyo dial gauge.

A previous study has developed a model of the laser milling process and a set of guidelines have been developed to assist the characterisation of the laser ablation trials⁴. This is dependant on knowing the material characteristics shown in Table 2.

| Characteristic | Units |
|--------------------------------|----------------------------------|
| Thermal Conductivity | $\text{W m}^{-1} \text{K}^{-1}$ |
| Density | g cm^{-3} |
| Heat Capacity | $\text{J kg}^{-1} \text{K}^{-1}$ |
| Vaporisation temperature | K |
| Specific heat of vaporization | kJ kg^{-1} |
| Reflectivity of target surface | % |

Table 2: Material characteristics required for modelling of laser milling process.

Minimum Pulse Irradiance. For a given laser pulse width and given material properties the minimum irradiance required to cause vaporization can be determined. Using a lower irradiance at this pulse width will have no material removal effect as the vaporisation temperature has not been reached. Therefore finding this threshold irradiance provides a processing boundary condition.

As the laser repetition rate is increased from minimum to maximum, the pulse width increases whilst the irradiance and pulse energy decreases. Therefore determining the threshold irradiance identifies a maximum repetition rate limit. Generally this indicates the highest removal rate that can be achieved. Lower laser repetition rates can still remove material when the pulse irradiance is above the minimum limit, however the pulse irradiance has an upper limit that is governed by the generation of laser-induced absorption waves (LAW) which block the delivery of the beam to the target^{6,7}. There are

several different types of LAW which have different characteristics depending on the pulse irradiance, and in this case the upper limit of removal is limited by laser-supported detonation.

2.1 Laser Milling of Polycrystalline Diamond

The ablation characteristics of PCD were investigated by a matrix of tests which varied specific laser parameters and measured material removal rates in a 2 mm by 2 mm area, as shown in Figure 1.

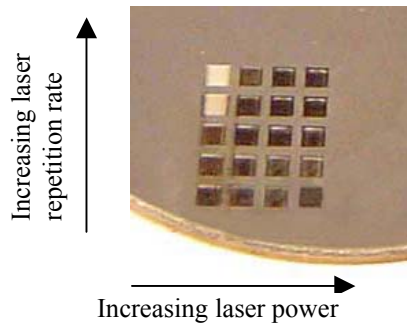


Figure 1 : Polycrystalline diamond milling test matrix

Different pulse repetition rates were selected and the output power was adjusted using the variable optical attenuator to produce a range of operating intensities. The maximum laser pulse characteristics for varying laser repetition rates for both sets of milling trials is shown in table 3.

| Laser Rep. Rate [kHz] | Pulse Irradiance [W/cm^2] | Pulse Energy [mJ] | Pulse Width [nsecs] |
|-----------------------|---|-------------------|---------------------|
| 10 | 1.5×10^9 | 13 | 47 |
| 20 | 6.2×10^8 | 7.4 | 63 |
| 30 | 3.1×10^8 | 5.0 | 86 |
| 40 | 1.7×10^8 | 3.8 | 120 |
| 50 | 1.1×10^8 | 3.1 | 156 |

Table 3 : Laser pulse characteristics for milling trials

For each test in the matrix the laser pulse width, irradiance, and ablation time were recorded. Ablation depth measurements were used to calculate the volume of material removed and removal rate. Figure 2 shows the results of the PCD laser milling trials.

The PCD was comparatively easy to ablate, with almost all tests removing an appreciable amount of material. The results show that higher repetition rates produce the fastest rate of removal. It was also noted that the base of the milled area became smoother as the laser repetition rate was increased. This result determined the best laser milling conditions and showed that a high power nanosecond-kHz operating regime is effective for milling PCD.

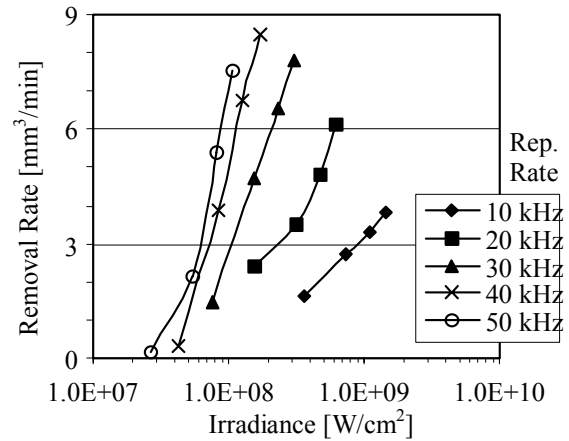


Figure 2: Results of polycrystalline diamond laser milling trials⁸

2.2 Laser Milling of Tungsten Carbide

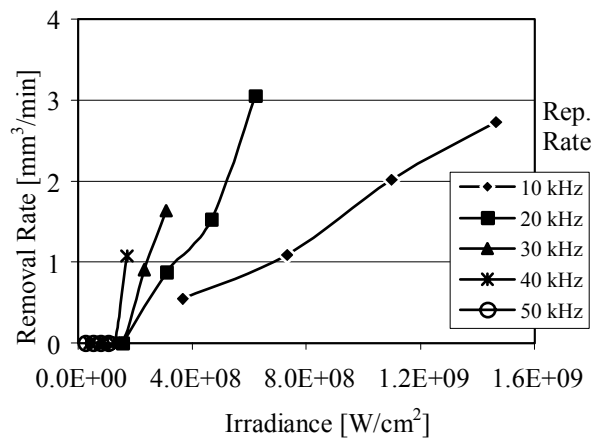


Figure 3: Results of WC laser milling trials⁸

The same method was used for the laser milling trials of WC. The WC material was on the reverse side of the disc used in the PCD trials above. The results are presented in Figure 3.

The results show much lower removal rates than for PCD. Lower laser repetition rates (which have high

pulse irradiance) produce higher removal rates – whereas the highest repetition rate of 50 kHz cannot be used for ablation at the available pulse irradiances since there is no material removal at all. The highest removal rates occur in the 10-20 kHz range and are discussed below.

2.3 Modelled and Experimental Results for Polycrystalline Diamond

A model for laser milling has been developed which has proven to be an effective tool in the search for optimised operating conditions. It makes the simplifying assumption that each laser pulse acts in two stages : a melting stage where the surface of the work-piece is raised to the vaporisation temperature, followed by a material removal stage where vaporisation occurs in a controlled manner. This is illustrated in Figure 4.

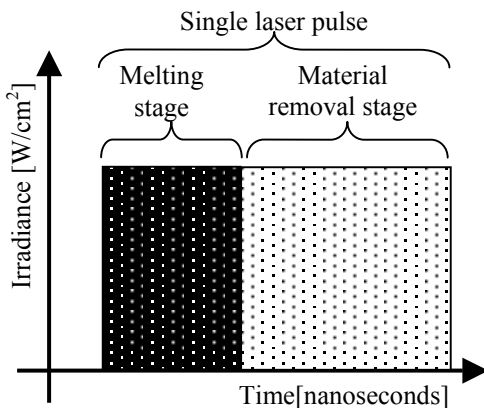


Figure 4 : The representation of a laser pulse for the milling model.

Using initial conditions of the material characteristics (as shown in Table 2) and the experimental laser pulse characteristics, the model initially calculates the duration of the melting stage and then determines the material removed by the remainder of the pulse, leading to a predicted removal rate.

PCD is composed of many diamond particles bonded together with a cobalt binding agent. In order to apply the laser milling model to this material, a set of material properties have to be determined, but in the case of PCD this becomes difficult because it is a composite material. Therefore a simplifying assumption must be made for the purposes of this model that PCD comprises only of diamond. This is not such a gross assumption given that the cobalt binder is a small percentage of the overall PCD weight².

Diamond is kinetically stable but not thermodynamically stable^{9,10}. This means that as the temperature of the diamond increases, it converts to graphite. Since both diamond and graphite are different lattice arrangements of carbon, the thermodynamic and kinetic relationship between them is shown in the phase diagram for carbon, which is shown in Figure 5. Note that in this figure the diamond used in PCD is referred to as Catalytic HPHT (High Pressure High Temperature) synthesis diamond.

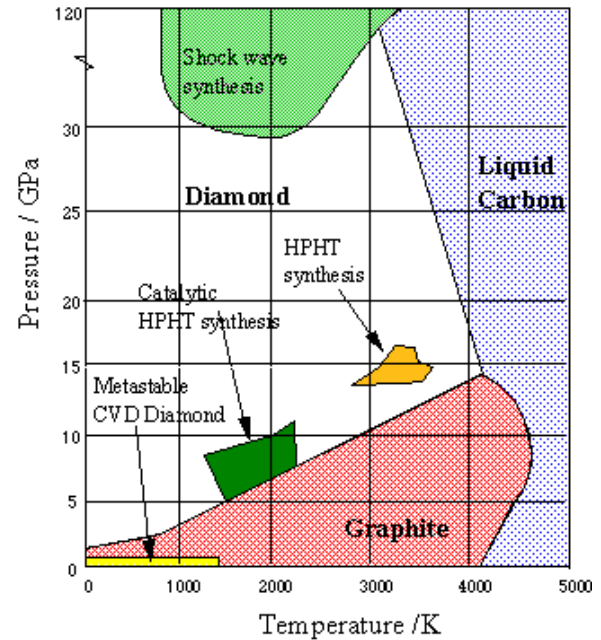


Figure 5 : Phase diagram for carbon¹⁰

The material properties for diamond and graphite are shown in Table 4. Note that there are significant differences between the two materials, particularly thermal conductivity and density. The model was augmented for this change in material properties by using a two stage approach : for each laser pulse, the PCD initially has the material characteristics of diamond until the temperature reaches 1000°C (where the diamond changes to graphite), and then for the rest of the pulse duration the material characteristics of graphite are used.

The results of the modelling work for PCD are reproduced in Figure 6 alongside the experimental results. For higher repetition rates there is a good correlation between modelled and experimental results, however, at lower repetition rates there is a difference. This could be due to over simplification of the model, since it doesn't take into account any effects of the laser pulse shock wave (and the

consequent change in pressure) or any other laser pulse effect which could affect the conversion of diamond to graphite. Consequently the material characteristics used in the model may not be the same as the target material, which could cause modelling errors. In addition the laser pulse shockwaves are larger at higher irradiance pulses which may explain why the error increases as the irradiance increases.

| Characteristic | Units | Diamond | Graphite |
|-------------------------------|----------------------------------|---------|-----------------------|
| Thermal Conductivity | $\text{Wm}^{-1} \text{K}^{-1}$ | 540 | 24 to 85 ^a |
| Density | g cm^{-3} | 4.13 | 2.25 |
| Heat Capacity | $\text{J kg}^{-1} \text{K}^{-1}$ | 0.512 | 0.7 |
| Vaporisation temperature | K | n/a | 5100 |
| Specific heat of vaporization | kJ kg^{-1} | n/a | 59600 |

^a Note that this depends on the crystal lattice orientation and has a range of typical values.

Table 4 : PCD modelling parameters^{11,12}

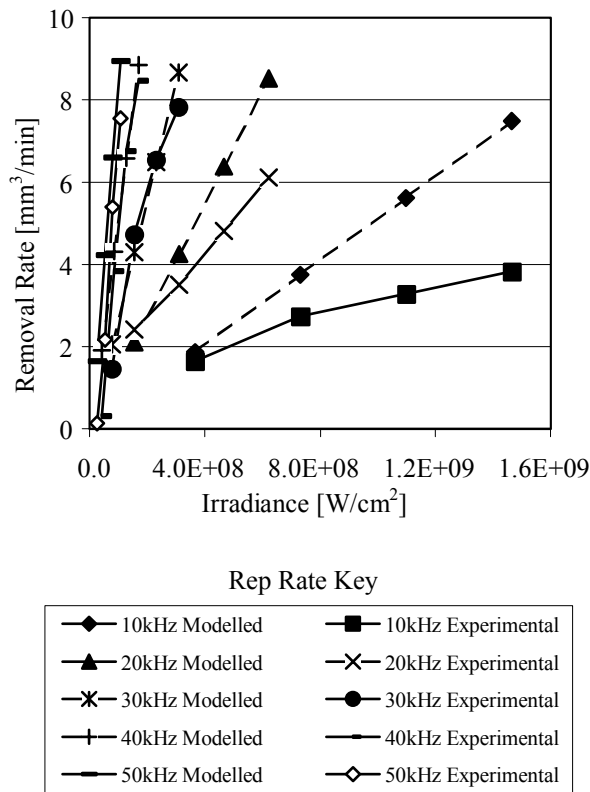


Figure 6. Experimental and predicted material removal rates for polycrystalline diamond.

The experimental results show a higher removal rate for PCD at higher repetition rates and the model can be used to understand why this happens. Figure 7 shows a selection of the results of the PCD modelling work (note that this figure only shows the case at the maximum available irradiance for each laser repetition rate). The figure shows that for all laser repetition rates the melting stage is a small proportion of the total pulse length, leaving a large removal stage. During the removal stage the penetration velocity is proportional to the pulse irradiance⁶, so the “Removal Stage” shaded area of each pulse in the figure is an indication of the relative volume removed per pulse. It can be seen from the figure that the largest area (and therefore the most material removed) is at lower repetition rates, however this is for a single pulse only. When the laser repetition rate is taken into account (i.e. in any given period of time there are 5 times more pulses at 50 kHz than at 10 kHz) the model shows that the removal rate is slightly higher at higher repetition rates.

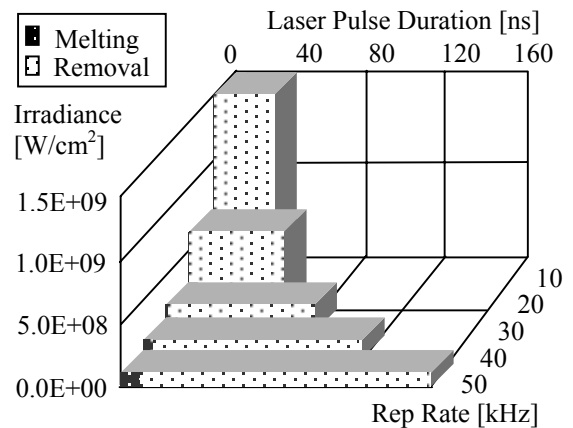


Figure 7. Modelling results for PCD

2.3 Modelled and Experimental Results for Laser Milling Tungsten Carbide

The results of the modelling work for WC are reproduced in Figure 8 alongside the experimental results. The experimental results show that as the laser repetition rate increases the removal rate decreases, which is predicted by the modelled results. The model shows why this is the case. Figures 9a and 9b show the predicted material removal for two cases – firstly the case of 50kHz where there was almost no material removal and secondly the case of 30kHz where there was considerable success. Both figures show four laser pulses (labelled A to D), which have 25, 50, 75 and 100% of maximum available

irradiance respectively, and both figures use the same scales on all axes.

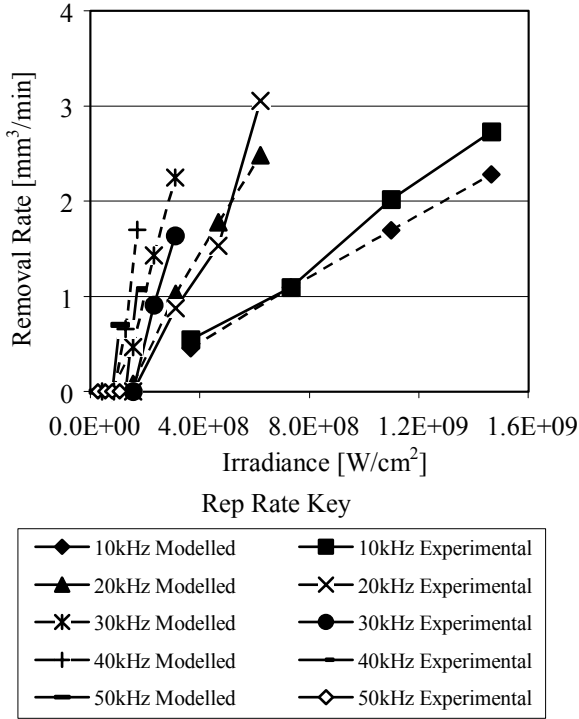


Figure 8. Experimental and predicted material removal rates for WC.

For the 50kHz case (Figure 9a), it can be seen that although the pulses are relatively long the pulse irradiance is low, and for three cases the vaporisation temperature is not reached within the pulse duration. Only the maximum pulse irradiance reaches the material removal stage.

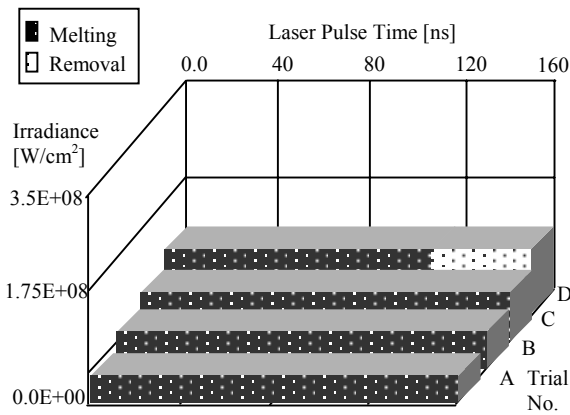


Figure 9a. Predicted material removal for laser milling tungsten carbide at 50 kHz repetition rate

However for the 30kHz case (Figure 9b) it can be seen that whilst the pulse durations are shorter, the pulse irradiance is much higher and the material removal stage is reached in three cases.

The model shows why the removal rate drops to zero at 50kHz repetition rate for 3 out of 4 cases – the pulse irradiance is insufficient for the material to reach its vaporization temperature, so there is no vaporization and therefore no material removal. This means that the minimum pulse irradiance boundary condition is not reached. Only at lower repetition rates is material removed where the pulse irradiance level is high enough to reach the vaporization temperature within the duration of the pulse.

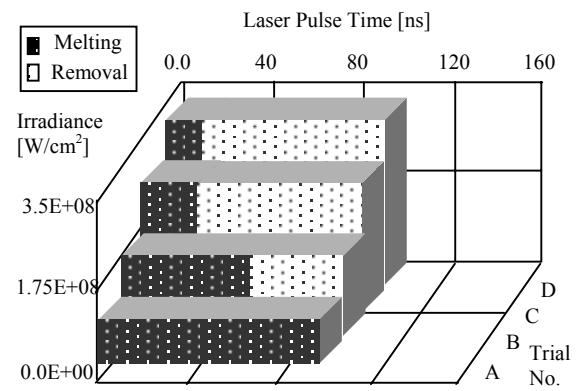


Figure 9b. Predicted material removal for laser milling tungsten carbide at 30 kHz repetition rate

It is interesting to note that for both of these test cases the laser output power was the same. This means that by maintaining the laser output power and by changing other laser parameters a great deal of improvement to the material removal rate can be made.

If the laser repetition rate is further decreased below 10kHz then the removal rate may not correspondingly increase. As the repetition rate decreases the laser pulse irradiance increases and at these higher irradiances Laser-Induced Absorption Waves are produced which can absorb and block the pulse^{6,7}. This has the effect of reducing the incident pulse irradiance onto the target and could consequently reduce the removal rate.

3. Laser Cutting PCD Cutting Tool Blanks

All of the laser piercing and cutting trials used the higher power Starlase AO4 Nd:YAG Q-switched DPSSL at the fundamental wavelength of 1064 nm. This pulsed laser offers average powers up to 420 W

at a range of repetition rates and pulse durations between 3 to 50 kHz and 20 to 200 ns respectively. The output beam power was varied using a proprietary attenuator unit, collimated with a Galilean telescope and then directed into an Anorad XYZ motion stage. This stage moved the target in the XY directions and the focussing head in the Z direction. The Anorad system is granite mounted and has linear drives capable of a top speed of 2 m/s with an accuracy of $\pm 1 \mu\text{m}$ over an XY travel of 450 x 450 mm. The laser beam was focussed with a lens of focal length 149 mm which produced at best focus a $\text{\O}200\mu\text{m}$ focal spot. The cutting head allowed a co-axial gas jet to be used to assist the cutting process which could be either compressed air, oxygen or nitrogen and could be supplied to the work-piece at pressures up to 10 Bar.

There are a number of different ways that laser beams can be used to cut sheet materials. Research has identified 7 distinct cutting mechanisms^{13,14}:

- Vaporisation Cutting – material removal by vaporisation.
- Fusion Cutting “Melt and blow” – the laser beam creates a melt pool and a co-axial gas jet blows the liquid out of the bottom of the cut.
- Reactive Fusion Cutting “Melt, burn and blow” – similar to fusion cutting except that the co-axial gas jet reacts exothermically with the molten material, adding another heat source to the process.
- Thermal stress cracking – the process of creating a controlled thermal fracture steered by the laser through the material. Only applies to very brittle materials, typically glass.
- Scribing – the process of making a groove or line of holes in the material sufficient to weaken it so that it can be mechanically broken.
- Cold Cutting – this process uses ultra-violet wavelength light to break molecular bonds within organic materials. There is no heat affected zone.
- Laser assisted oxygen cutting – this process uses the laser as a heat source to ignite the metal in an oxygen stream, and is used for cutting thick section steel.

Since four of these cutting mechanisms (thermal stress cracking, scribing, cold cutting and laser assisted oxygen cutting) require specific materials and/or laser wavelengths, they do not apply to the cutting of PCD blanks. The remaining three cutting techniques (vaporisation cutting, fusion cutting and

reactive fusion cutting) can be considered as potential cutting solutions and are investigated below.

The laser cutting process must produce a cut that enables the PCD to be used as a cutting tool. This is shown in figure 10 and also illustrates the required sharp edge on the diamond side of the PCD material. This edge must be very straight and have as small a radius as possible. The sharp cutting edge is only required on the cutting face and not on the other sides of the PCD part.

As described in the introduction, laser processing has two applications for PCD cutting tools. The first application is initially cutting the tool to the required shape and the second is maintaining the sharp cutting edge, which involves trimming the cutting face.

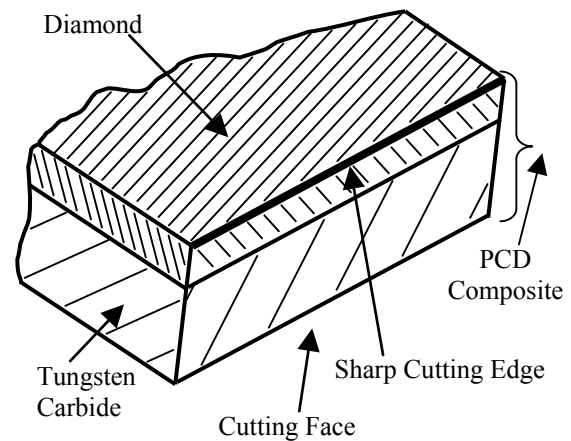


Figure 10 : The sharp cutting edge of the PCD cutting tool.

3.1 Laser Cutting of PCD by Vaporisation

A process speed for vaporisation cutting can be estimated by considering the volume removed in order to create the cut. Using the removal rate data obtained from the laser milling trials and estimating a cut width (known as the kerf width), a cutting speed can be obtained.

For a 1.6 mm thick sheet of PCD, estimating the Kerf width to be 150 microns and using the same laser as for the milling trials it is estimated that the cutting speed would be around 12.5 mm/min.

Practical trials were attempted in a similar fashion to the laser milling trials using a laser and scanner, with the exception that the programmed shape was a line rather than a square. The laser beam was repeatedly

scanned onto the WC side of the PCD in an attempt to produce a slot type cut.

The results were poor and the cut did not penetrate through the material thickness. It was found that a “Vee” shaped groove had been milled into the material but there was little depth (less than 25% of the material thickness) and at the bottom of the Vee shape there was a lot of recast material. There was no penetration through to the other side of the PCD. Extending the duration of these trials (i.e. the equivalent of slowing down the overall cutting speed) had no effect on the depth of cut.

The explanation for this (noting that the focus is fixed onto the original top surface of the work-piece and does not change) is as follows : initially the laser milling is successful and material is removed from the work-piece. As a “Vee” groove is created, the incident surface progressively moves downwards, further away from best focus causing the size of the focal spot to increase and therefore laser pulse irradiance to dramatically decrease. This cutting process is therefore self-limiting.

As seen in figure 3, WC has a high threshold of laser irradiance needed to remove material by vaporisation so the focal spot only has to increase by a small amount before the pulse irradiance drops below this vaporisation threshold level. From this point in the test there is no material removal - all of the energy from the laser beam now goes into creating a melt pool and heating up the work-piece.

This effect can be demonstrated by considering the removal rate at either end of the Rayleigh range (which is distance between the points where the area of the focal spot is twice that at best focus, i.e. an increase in beam radius of $\sqrt{2}$). Referring to Figure 3 (Removal Rate characterisation for WC), consider the laser operating at 10 kHz and at full power with best focus fixed on the initial surface of the work-piece. At the start of the test the focal spot size is at best focus and the removal rate is at it's highest (in this case $2.7 \text{ mm}^3/\text{min}$). As material is removed the work-piece surface moves away from focus, and the focal spot increases. At the end of the Rayleigh range ($390 \mu\text{m}$ below the initial work-piece surface and best focus), the focal spot is twice that of best focus, the pulse irradiance is halved and the removal rate drops by 60%. As more material is removed the removal rate drops even more.

This cutting method cannot be used to cut PCD cutting tools. Moving the laser beam focus downwards during the cutting process does not work because when the beam focus is positioned at the

bottom of the cut the beam would clip and damage the top surface of the PCD blank disk.

3.2 Laser Cutting of PCD by Fusion Cutting

These trials involved the use of an XYZ positioning stage with a gas-assisted cutting head as previously described. The laser used for these trials was the Starlase AO4 with a maximum output of 420 W. In order to perform true “Melt and Blow” trials the assist gas used must be inert to avoid any reactions with the PCD, so nitrogen was chosen as a cost-effective relatively inert assist gas.

“Melt and Blow” laser cutting involves the use of the laser beam to create a molten pool of material and for the co-axial gas jet to blow this liquid out of the bottom of the cut. This method has the potential to produce high quality cutting with excellent perpendicular edge quality. This type of laser cutting has two distinct phases :

Pierce-through Phase : occurs at the start of a cut-line where a percussion drilled hole is made. For most of this operation the hole is blind and the debris from the drilling operation is thrown up out of the hole entrance, resulting in an area of dross on the material surface around the hole.

Cutting Phase : follows the pierce-through. The laser cutting head is moved over the material at a constant speed and the material is cut in a single pass. An angled cut front is established and this is where the laser beam is absorbed. The laser beam is waveguided through the thickness of the material but the process is complicated and involves two mechanisms operating in parallel¹³ – Fresnel absorption and plasma absorption and re-radiation. The key to this process is how well the molten material adheres to the solid part of the work-piece and the ability of the gas jet to remove it. This issue is further complicated by the effects of the gas jet velocity inside the cut-slot and the problems of Mach pressure gradients within the high pressure gas jet.

A matrix of pierce-through tests were performed to find the best settings for cutting trials. Pulse repetition rates from 3 to 30 kHz were investigated with irradiances ranging from $100 \text{ MW}/\text{cm}^2$ to over $2.6 \text{ GW}/\text{cm}^2$. The assist gas pressure was varied from 1 to 8 Bar.

None of the tests in the matrix successfully pierced the PCD even when the matrix was extended to include longer duration tests. Examination of the test matrix revealed a similar situation to vaporisation cutting – holes of limited depth with a lot of melted

and resolidified material at the bottom. It was noted that higher repetition rates had deeper holes than lower repetition rates.

We suggest that a combination of effects prevented successful fusion cutting, firstly the “focal spot-size vs depth” issue, as previously described for vaporisation cutting, which was limiting the effectiveness of the laser beam as it penetrated into the PCD, and second the strong cooling effect produced by the high velocity gas jet (also exaggerated by the effect of the pressure-drop across the cutting nozzle).

3.3 Laser Cutting of PCD by Reactive Fusion Cutting

This method of laser cutting is very similar to “Melt and Blow” laser cutting except that the assist gas used reacts exothermically with the molten material and becomes another heat source, accelerating the creation of the melt-pool and therefore increasing the cutting speed. The reactive gas in this case is oxygen, so two candidate assist gases were considered – oxygen and air. The extra processes involved with the reaction occurring at the cut-front make the cutting process more complicated.

In order to determine the best laser cutting parameters, the development process was split into two sections: pierce-through tests and cutting trials.

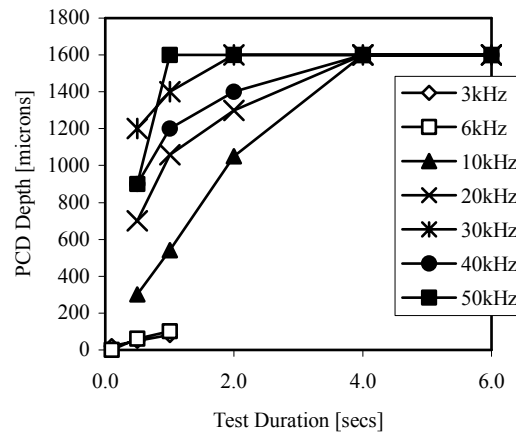
Pierce Through Tests Using Air as Assist Gas

A test matrix of pierce-through tests was devised using air as the assist gas, varying repetition rate and test duration. Laser power was kept at maximum throughout. Figures 11 and 12 show a photograph and graph of the results. It was found that the quickest pierce-through was achieved at the highest laser repetition rate and maximum power. The pierce-through took 1 second with laser parameters of 350 W at 50 kHz with a peak irradiance of 110 MW/cm².



Figure 11: Pierce-through test matrix with air assist gas.

Pierce-Through Tests using Oxygen Assist Gas



A matrix of pierce-through tests using oxygen assist gas was completed varying the assist gas pressure and the test duration time. The laser parameters were maintained at full power and maximum repetition rate using the best laser settings from previous pierce-through trials. The matrix showed that at 4 Bar gas pressure the pierce time was up to 2.5 times longer using oxygen but the process was noted to be much more vigorous. One explanation for the poor pierce-through times could be that the oxygen is creating more of a surface reaction and thus creating more heat which creates a melt-pool inside the material. If the assist gas jet does not have sufficient mechanical energy to blow the melt-pool up and out of the blind hole, adding more heat (laser beam and/or oxygen) will only cause the melt-pool to expand, preventing further penetration into the material. Subsequently the assist gas pressure was increased to 8 Bar and a noticeable improvement was seen, with pierce-through times comparable to that of the 4 Bar air assist gas times.

The results of the pierce-through tests indicated two prospective areas for laser cutting trials - keeping the laser parameters the same and using either air or oxygen as the assist gas at high pressure (8 Bar). Both of these areas used the same laser parameters – 50 kHz repetition rate, 350 W (full power at this repetition rate).

Cutting tests started with low speeds (10 mm/min) and were stepped up to 36 mm/min. Each test attempted to cut out a 2 mm square. It is preferable to operate at higher speeds because not only does this increase production rates but it also allows less time for the heat to diffuse sideways and creates narrower Heat Affected Zones (HAZ).

Cutting trials with air assist gas

The cutting trials with air assist gas did not manage to fully cut through the material. At slow speeds (10 mm/min) there was limited evidence of the cut on the reverse side of the material meaning that in certain places the cutting process had completely penetrated but not for the whole of the cut path. The 2mm square test part could not be removed.

Cutting trials with oxygen assist gas

These tests were more successful and many of the test squares could be removed from the PCD sheet, indicating a successful cut. Figure 13 shows cut-edge detail from one of these tests.

Clearly displayed in the diamond section of these cuts are striations, which are a characteristic of fusion and reactive fusion cutting. The cutting speed was increased to the point where the cutting process failed to penetrate through the PCD material. There was a sharp transition between cutting speeds that achieve penetration and those that did not. Once the gas jet could no longer eject molten material through the bottom of the cut the “melt, burn and blow” fusion cutting process did not work.



PCD Tungsten Carbide

Figure 13 : Edge detail using oxygen assist gas at 14 mm/min.

The optimum speed range was found to be 21 to 27 mm/min with the best edge quality obtained around 24 mm/min. Figure 14 shows the typical edge quality achieved. The assist gas jet was found to affect the edge quality of the cut and it is believed that a carefully designed nozzle will greatly improve both the cutting speed and the edge quality.

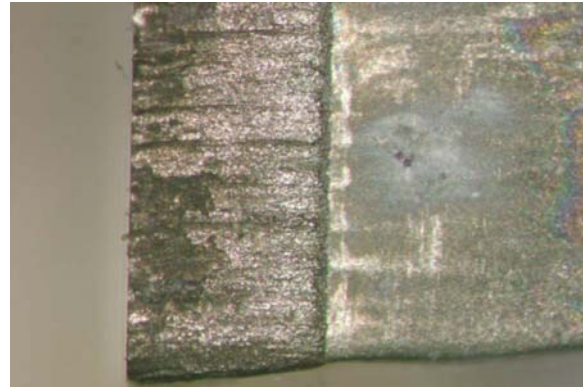


Figure 14 : Edge quality at optimum speed

The diamond layer of the PCD cutting tool blank is much easier to process than the WC layer. This can be easily seen by comparing the results of Figure 2 (removal rate characterisation of PCD) with Figure 3 (removal rate characterisation of WC). At 100 MW/cm² the PCD removal rate is 7.6 mm³/min whilst WC is just at the threshold of removal. For cutting purposes it means that the best cutting is with the WC side upwards, closest to the cutting nozzle and best focus. Trials confirmed this was the case.

3.4 The Reactive Fusion Laser Cutting Mechanism

The reactive fusion cutting process works when the high irradiance, high repetition rate laser pulses produce carbon (through the conversion of diamond into graphite) for the oxygen assist gas to react with as shown in Equation 1.



(where $\Delta H_c = -390.4$ kJ/mol)

This combustion process is exothermic⁹ and provides another heat source to increase the cutting speed. The pulse irradiance used in the successful cutting trials (120 MW/cm²) is just above the threshold for WC removal by vaporisation. It has been suggested that the cutting process is being enhanced by this vaporisation, with the oxygen assist gas reacts directly with the graphite vapour rather than the melt. This could be more reactive, resulting in more heat and faster cutting. There may also be a reaction between the oxygen assist gas and the WC. The details of this reaction are unknown but it may involve carbon being released from the WC and a similar exothermic reaction may take place as for the case of PCD, further increasing the speed of cut. Clearly the interaction between the laser pulse, the assist gas and the target material is an area for further investigation.

3.5 Cutting Edge Quality

The final process optimisation was to make the PCD cutting edge as straight and true as possible. The best settings for general PCD laser cutting (repetition rate 45 kHz, power 300 W, pulse energy 6.7 mJ, peak irradiance of 120 MW/cm²) produced a cutting speed of 24 mm/min but did not produce a cutting edge of sufficient sharpness and accuracy since reactive fusion cutting produces striations on the cut-face.

A laser polishing procedure was introduced to produce a sharp cutting edge on the diamond cutting face. This process is currently in development but early results shown in Figure 15 have produced finishes close to those produced by traditional EDM methods which are shown in Figure 16.

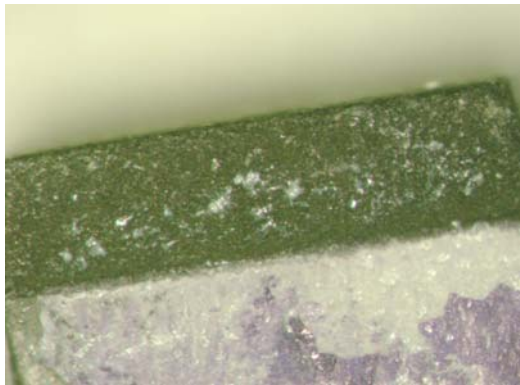


Figure 15 : Laser cut PCD with polished edge.



Figure 16 : EDM polished edge

A section of the laser cut edge was required to examine the quality of the laser processing and to determine the amount of damage and recast near the cut. Obtaining the section proved to be difficult, since the PCD composite material is not easy to cut, so the

section was made by EDM electro-discharge grinding.

A magnified view of part of the section centred on the PCD-WC interface is shown in figure 17, where the PCD is shown at the top and the WC is below. The sectioned view shows no discernable recast zone for either material. In the case of PCD this is understandable since there is a conversion of diamond to graphite during the ablation process – diamond has no liquid phase, so there is no way to form a recast layer, and the graphite is very soft and could easily be removed by the high pressure assist gas. In the case of WC, there is also no measurable recast layer. There are a number of explanations for this, with one possibility being that the amount of melted material is minimised due to the nanosecond laser pulses, which have been shown to be able to vaporise the WC. The vapour reacts with the assist gas and is then blown out of the cut zone.

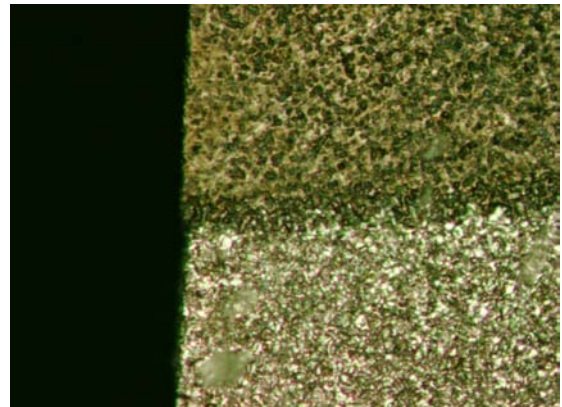


Figure 17 : Section view of the laser cut edge (magnification x 20)

Conclusions

Laser Milling:

Experimental results in this paper show accurate and controlled laser ablation of PCD and WC with high power pulsed DPSS lasers. The removal rates were characterised for both PCD and WC and it was shown that while PCD can be milled with high laser repetition rates, WC cannot, which leads to an understanding of how the laser pulse characteristics affect material removal rates.

Laser cutting:

The laser cutting mechanism of the PCD cutting tool blank was investigated with particular attention to the WC layer, since the PCD is comparatively straightforward to process. Using oxygen as a reactive assist gas to aid the cutting process has

resulted in cutting speeds which are industrially attractive. It was determined that the cutting mechanism is Reactive Fusion Cutting (commonly known as “Melt, Burn and Blow”) and the optimum parameters for general laser cutting were determined. However, further work is required to understand the interaction between the laser pulse, assist gas and material being cut.

Laser processing of PCD tooling blanks has two applications – cutting the raw blanks to shape and maintaining the sharpness of the cutting tools as they wear. It was shown that laser cutting of PCD is possible with DPSS lasers at much higher cutting speeds than alternative technologies. Laser polishing the “Sharp Cutting Edge” onto the PCD tool is an area currently under development.

Laser cutting has the potential to be much more versatile in the manufacture of cutting tools as it has many advantages, including reduced access requirements, no lubrication required, no tool wear and omnidirectional cutting capability. These advantages will allow the development of new PCD cutting tool designs.

Acknowledgements

The authors would like to thank the Powerlase Applications Team for their assistance with this paper.

References

- [1] JR Untermahrer et al, “High peak power diode-pumped solid state lasers and industrial applications”, CLEO 1998 Technical Digest, Vol. 6, May 1998.
- [2] Element 6 Website, June 2004.
- [3] Q. Bai, Y. Yao, S Chen, “Research and development of polycrystalline diamond woodworking tools”, Int J Refractory Metals & Hard Metals, vol. 20 (2002), pp 395 –400.
- [4] Harrison P, Henry M, Henderson I, Brownell M, (2004) “Laser Milling of Metallic and Non-Metallic Substrates in the Nanosecond Regime with Q-Switched Diode Pumped Solid State Lasers”, High Power Laser Ablation 2004, Taos, New Mexico.
- [5] Matweb material property data website, June 2004

[6] Ready JF, (1997) Industrial Applications of Lasers, Academic Press, Chapter 12.

[7] Ready JF, (2001) LIA Handbook of Laser Material Processing, Magnolia Publishing, section 5.7.2

[8] Harrison P, Henry M, unpublished results from Powerlase Applications Lab, 2001 – 2004.

[9] University of Wisconsin-Madison, Department of Chemistry website, “Buckyballs, Diamond and Graphite”, April 2005.

[10] Bristol University Diamond Group website, March 2005.

[11] Pierson HO, (1993) Handbook of Carbon, Graphite, Diamond and Fullerenes – Properties, Processing and Applications, William Andrew Publishing

[12] MadSci Network website, Earth Sciences section, diamond properties, March 2005.

[13] Steen WM, (2003) Laser Material Processing, Springer-Verlag, Chapter 3.

[14] Powell J, (1998) CO₂ Laser Cutting, Springer-Verlag, Chapters 1 and 4.